Tunneling dynamics, symmetry, and far-infrared spectrum of the rotating water trimer. II. Calculations and experiments

E. H. T. Olthof, A. van der Avoird, and P. E. S. Wormer
Institute of Theoretical Chemistry, NSR-Center, University of Nijmegen, Toernooiveld, 6525 ED Nijmegen, The Netherlands

Kun Liu and R. J. Saykally
Department of Chemistry, University of California, Berkeley, California 94720

(Received 24 April 1996; accepted 6 August 1996)

With the Hamiltonian derived in the preceding paper and the *ab initio* potentials of T. Bürgi, S. Graf, S. Leutwyler, and W. Klopper [J. Chem. Phys. **103**, 1077 (1995)] and of J. G. C. M. van Duijneveldt-van de Rijdt and F. B. van Duijneveldt [Chem. Phys. Lett. **237**, 560 (1995)], we calculate the pseudo-rotation tunneling levels in a rotating water trimer. The internal motions are treated by a three-dimensional discrete variable representation and the Coriolis coupling with the overall rotation is included. Also the effects of donor tunneling are included, by introducing semi-empirical coupling matrix elements. New experimental data are presented for the *c*-type band at 87.1 cm^{-1} in $(H_2O)_3$, which show that specific levels in the donor tunneling quartets of this band are further split into doublets. With the results of our quantitative calculations and the model of the preceding paper we can understand the mechanisms of all the splittings observed in the earlier high-resolution spectra of $(H_2O)_3$ and $(D_2O)_3$, as well as these new splittings, in terms of pseudo-rotation tunneling, donor tunneling and Coriolis coupling. An unambiguous assignment is given of all the bands observed and analyzed. The *ab initio* potential of the Van Duijneveldts yields accurate energies of the lower pseudo-rotation levels, the potential of Bürgi *et al.* performs better for the higher levels. With our analysis we can deduce from the spectra that donor tunneling involves inversion of the trimer. © *1996 American Institute of Physics.* [S0021-9606(96)01642-X]

I. INTRODUCTION

Several far-infrared transitions in $(H_2O)_3$ and $(D_2O)_3$ have been measured in high resolution, both at Berkeley[1–4] and by Suzuki and Blake.[5] Most of the data refer to $(D_2O)_3$. The first band measured by Pugliano and Saykally[1] is a *c*-type transition at 89.6 cm^{-1}, which is strongly perturbed and now believed[2] to be a hot band. Subsequently, two more bands were reported, a *c*-type transition at 41.1 cm^{-1} (Ref. 5) and an *a*-type transition at 98.1 cm^{-1}.[2,3] Finally, an *a*-type transition has been found[3] at 82.5 cm^{-1}, but this band could not yet be assigned in detail. For $(H_2O)_3$ a *c*-type transition at 87.1 cm^{-1} has been reported and analyzed by Liu *et al.*[2,3]

It is believed that the frequencies of these transitions correspond to the intermolecular vibrations in these trimers, in particular to the pseudo-rotations (or flipping or torsional vibrations) of the external protons. In most of the spectra it has been observed that the rovibrational transitions are split into quartets. Liu *et al.*[2] have demonstrated that the splittings in these quartets are caused by donor tunneling and that the effective permutation-inversion group of the water trimer is G_{48}. We will show in the present paper, for the $(H_2O)_3$ band at 87.1 cm^{-1}, that part of the lines in the quartets are further split into doublets.

The first theoretical treatment of the pseudo-rotation tunneling dynamics is the calculation by Schütz *et al.*[6] These authors used a one-dimensional model that flips one of the three external protons at a time; the potential along this path is obtained from *ab initio* calculations. Two- and three-dimensional model computations for the pseudo-rotation tunneling or torsional motions were subsequently performed by Klopper *et al.*,[7] by Sabo *et al.*,[8] and by Meijer *et al.*[9] They all used three-dimensional potential surfaces fitted to *ab initio* calculations and a kinetic energy operator for the pseudo-rotation tunneling which was postulated *ad hoc*. The three-dimensional calculations by Sabo *et al.*[8] and by Meijer *et al.*[9] needed no further simplifications, but in the model calculation of Klopper *et al.*[7] the three torsional coordinates were transformed into hyperspherical coordinates and the hyperspherical radius R was frozen. The three-dimensional kinetic energy operator was transformed to the two hyperspherical angles and the effective rotational constant F was treated as an empirical parameter. Both the parameters R and F were then fitted by an adjustment of the calculated levels to the measured far-infrared frequencies.

A theoretical treatment of the pseudo-rotation as well as of the donor tunneling (also called bifurcation tunneling) in the water trimer was given by Wales.[10] He investigated various tunneling pathways by scanning the potential surface, for which he used both an empirical and an *ab initio* potential. Then he applied a Hückel type model with tunneling matrix elements β_1, β_2, and β_3 for the three relevant rearrangement pathways that he found, to describe the corresponding tunneling levels and splittings. Gregory and Clary[11,12] also presented a treatment that includes both pseudo-rotation and donor tunneling. These authors used the elaborate H_2O-H_2O pair potential of Millot and Stone,[13] with some three-body terms added in their second paper,[12] and de-

scribed all 12 intermolecular degrees of freedom by the diffusional quantum Monte Carlo method. By making a fixed-node approximation and correlated sampling of ground and excited states, they computed a typical frequency for the pseudo-rotation and another much smaller one for the donor tunneling. These frequencies have the correct order of magnitude, when compared with the observed splittings, and their ratios for $(H_2O)_3$ and $(D_2O)_3$ are realistic as well.

None of the previous theoretical treatments included the overall rotation of the water trimer. In the preceding paper (paper I) a kinetic energy operator was derived for pseudo-rotation tunneling in a rotating trimer. It contains the terms found in the Hamiltonians used in the previous calculations,[7–9] but with an explicit expression for the effective moments of inertia associated with the monomer torsions. Moreover, it includes additional terms that do not depend on the overall trimer rotation, as well as the Coriolis coupling between the trimer rotation and the torsional motions of the monomers. Then, a qualitative model was developed for the eigenstates of this Hamiltonian, in which the symmetry group G_6 was used to simplify the description of the pseudo-rotation tunneling. This model was extended by introduction of the donor tunneling, with the symmetry group G_{48}, and an analysis of the combined effects of donor tunneling and Coriolis coupling.

In the present paper (paper II) we present quantitative, non-empirical, calculations. To describe the three-dimensional pseudo-rotation dynamics we use the discrete variable representation (DVR) method and two different potentials extracted from *ab initio* calculations.[14,15] The eigenvalues yield the large tunneling splittings associated with the pseudo-rotation; the relevant Coriolis coupling constants are computed from the corresponding eigenfunctions. When extending the quantitative model by including donor tunneling, we use empirical values for the donor tunneling matrix elements. From the partly empirical Hamiltonian matrix so obtained we get the complete level splitting pattern, for any given value of J. Then we compare the predictions of our qualitative and quantitative models with the experimental spectra.

II. QUANTITATIVE CALCULATIONS

A. Method

Since we will frequently refer to the equations in paper I, we denote these equations as Eq. (I.x). The equations in the Appendixes A, B, and C of paper I will simply be indicated with A, B, or C, because no confusion is possible in this case.

In our quantitative computation of the pseudo-rotation tunneling states that correspond to the flipping of the three external protons, in combination with the overall rotation of the trimer, we used the complete kinetic operator from Eq. (I.2) that was derived for this constrained three-dimensional internal motion, with only the approximation that we neglect the very small χ_ν-dependent terms in the effective inertia tensor of Eqs. (I.4) and (A37). With the potential $V(\chi_A,\chi_B,\chi_C)$ this gives the Hamiltonian $H=H^{\rm int}+H^{\rm rot}+H^{\rm Cor}$ defined in Eqs. (I.8), (I.5), and (I.7). For the effective (vibrationally averaged) trimer rotational constants we took the values $A=B=0.221\ 72\ \text{cm}^{-1}$ for $(H_2O)_3$ and $A=B=0.193\ 34\ \text{cm}^{-1}$, $C=0.103\ 02\ \text{cm}^{-1}$ for $(D_2O)_3$ that have been determined[2] for the ground states of these trimers. These experimental values show that the vibrational averaging over the six equivalent asymmetric (C_1) equilibrium structures produces a nearly planar symmetric rotor. Since C has not yet been determined for $(H_2O)_3$ we assumed that it equals $A/2$. For the effective moment of inertia Λ of the monomers we used Eq. (I.3) and the principal moments of inertia $I_x=I_b$ and $I_y=I_a$ of H_2O and D_2O obtained from the equilibrium structures used in the *ab initio* calculations.[14,16] These values are very close to the vibrationally averaged values obtained from ground state rotational constants.[17] This gives an effective rotational constant $\hbar^2/(2\Lambda)$ for the constrained monomer rotation which is $21.39\ \text{cm}^{-1}$ for H_2O and $11.73\ \text{cm}^{-1}$ for D_2O. The angle ξ_A which defines the orientation of the monomer rotation axes with respect to the trimer frame (see Fig. 1 of paper I) was taken to be 130°[14–16], and the monomer angle φ_A is 55.49° for H_2O and 58.26° for D_2O.

The potential $V(\chi_A,\chi_B,\chi_C)$ is given by Bürgi *et al.*[15] as an analytic site-site potential with parameters fitted to their *ab initio* calculations. We used the BSSE-corrected modE-PEN parameters from Table I in Ref. 15, and refer to this potential as the BGLK-potential. The Van Duijneveldts[14] represent their potential by a power series in $\chi_A^{n_A}\chi_B^{n_B}\chi_C^{n_C}$ with $n_A+n_B+n_C\leqslant 6$ and coefficients from a least squares fit to their own *ab initio* calculations. We used a slightly improved form of this expansion[18] that is valid for a somewhat larger range of χ_ν values (from $-110°$ to $+110°$ approximately), and refer to it as the DD-potential. In both cases the angles that were varied in the *ab initio* calculations describe the rotations of the water monomers about an axis through their OH_1 bonds, whereas in the derivation of the Hamiltonian in paper I it was assumed that the monomers rotate about an axis through their center of mass and proton H_1. Without the latter assumption the Hamiltonian would have been considerably more complicated. There are two possible ways to deal with this problem. The first is to replace the effective moment of inertia Λ by the value that applies to a rotation of the monomers about their OH_1 bands—this would give $\hbar^2/(2\Lambda)=19.47\ \text{cm}^{-1}$ instead of $21.39\ \text{cm}^{-1}$ for H_2O—and assume that the form of the kinetic energy operator in Eq. (I.2) is still correct. The second possibility, which we have chosen, is to retain the correct value of Λ in the kinetic energy of Eq. (I.2) and assume that the potential $V(\chi_A,\chi_B,\chi_C)$ computed for the rotations about the OH_1 bands describes to a good approximation the rotations about the axes through the centers of mass. We believe that the inaccuracies present in the *ab initio* potentials $V(\chi_A,\chi_B,\chi_C)$ and in the model with just the constrained monomer rotations are of the same size as the error caused by this approximation.

For the overall rotations we used a basis of normalized symmetric top functions $|JKM\rangle=[(2J+1)/8\pi^2]^{1/2}\times D^{(J)}_{MK}(\alpha,\beta,\gamma)^*$ with fixed J and M, because these are ex-

act quantum numbers, and $K=-J,-J+1,\ldots,J$. The internal coordinates χ_A,χ_B,χ_C are described by the discrete variable representation (DVR) of Refs. 19 and 20. This DVR method consists of a $(2N+1)$-point quadrature for each variable x with points and weights $\{(x_n,w_n), n=-N,\ldots,N\}$ and a set of associated basis functions $\{\xi_n(x), n=-N,\ldots,N\}$ with the property that $\xi_n(x_i)=w_i^{-1/2}\delta_{ni}$. One proceeds in the same manner as in a variational calculation, except that the potential matrix elements are evaluated by quadrature. The use of this quadrature makes the potential, and any other operator which is a local function of the coordinates, diagonal in the associated basis. In the DVR method of Refs. 19, and 20 the quadrature points $x_n=n\Delta$ are equidistant, the weights $w_n=\Delta$ are equal to the grid spacing, and the associated basis functions are

$$\xi_n(x)=\Delta^{-1/2}\,\mathrm{sinc}\left[\pi\left(\frac{x}{\Delta}-n\right)\right]\equiv\Delta^{-1/2}\frac{\sin\,\pi\left(\frac{x}{\Delta}-n\right)}{\pi\left(\frac{x}{\Delta}-n\right)}. \tag{1}$$

The range of the variable x is from $-\infty$ to $+\infty$, but the wave function outside the points x_{-N} and x_N is effectively zero, which is equivalent to the assumption that the potential in this region is infinitely high.

We use this representation for each of the variables $\{\chi_\nu;\nu=A,B,C\}$. Actually these angular variables range from $-\pi$ to π, but the potential $V(\chi_A,\chi_B,\chi_C)$ becomes rather high at χ_ν values beyond $-\pi/2$ and $\pi/2$, so we may truncate the grid at about $\pm 110°$. With the potentials of Refs. 15 and 18 we obtain convergence of the lower eigenvalues of the operator H^{int} to within 0.01 cm^{-1} for a grid with boundaries at $\pm 112.5°$ and spacing $\Delta=7.5°$. The inaccuracy is mainly caused by the restriction of the boundaries, which could not be released for the DD-potential of Refs. 14 and 18, as the polynomial expansion of this potential begins to show spurious behavior for larger angles. The basis consists of product functions $\xi_{n_A}(\chi_A)\xi_{n_B}(\chi_B)\xi_{n_C}(\chi_C)$ and the matrix elements of the differential operators in H^{int} are

$$\left\langle \xi_{n_A'}(\chi_A)\xi_{n_B'}(\chi_B)\xi_{n_C'}(\chi_C)\left|\frac{\partial^2}{\partial\chi_A^2}\right|\xi_{n_A}(\chi_A)\xi_{n_B}(\chi_B)\xi_{n_C}(\chi_C)\right\rangle = \delta_{n_B'n_B}\delta_{n_C'n_C}\left\langle \xi_{n_A'}\left|\frac{\partial^2}{\partial\chi_A^2}\right|\xi_{n_A}\right\rangle \tag{2}$$

and similar expressions for B and C, with the one-particle integrals

$$\left\langle \xi_{n'}\left|\frac{\partial^2}{\partial\chi^2}\right|\xi_n\right\rangle=\begin{cases}-\dfrac{\pi^2}{3\Delta^2}, & \text{for } n'=n,\\[2ex] -\dfrac{2(-1)^{n'-n}}{(n'-n)^2\Delta^2}, & \text{for } n'\neq n.\end{cases} \tag{3}$$

The potential matrix elements are

$$\langle \xi_{n_A'}(\chi_A)\xi_{n_B'}(\chi_B)\xi_{n_C'}(\chi_C)|V(\chi_A,\chi_B,\chi_C) \times|\xi_{n_A}(\chi_A)\xi_{n_B}(\chi_B)\xi_{n_C}(\chi_C)\rangle = \delta_{n_A'n_A}\delta_{n_B'n_B}\delta_{n_C'n_C}V(n_A\Delta,n_B\Delta,n_C\Delta). \tag{4}$$

The matrix elements of the operators j_z, $j_\pm$ and their Hermitian conjugates, which occur in H^{Cor}, can be computed as follows. As described in paper I, the three-particle operators j_z, $j_\pm$ and their Hermitian conjugates reduce immediately to one-particle matrix elements. Thus from Eqs. (I.22) and (I.23) we see that $j_\pm$ gives rise to matrix elements $\langle\xi_{n'}(\chi)|\partial/\partial\chi|\xi_n(\chi)\rangle$, $\langle\xi_{n'}(\chi)|\cos\chi\partial/\partial\chi|\xi_{n'}(\chi)\rangle$ and from Eq. (A44) we find that we must evaluate $\langle\xi_{n'}(\chi)|\sin\chi\partial/\partial\chi|\xi_{n'}(\chi)\rangle$ for j_z. The latter two integrals are simplified by substituting a truncated resolution of identity—expressed in the sinc basis of Eq. (1)—between the function and the differential operator. The local functions $\sin\chi$ and $\cos\chi$ are diagonal,

$$\langle\xi_{n'}(\chi)|\cos\chi|\xi_n(\chi)\rangle = \delta_{n'n}\cos(n\Delta) \quad\text{and}\quad \langle\xi_{n'}(\chi)|\sin\chi|\xi_n(\chi)\rangle = \delta_{n'n}\sin(n\Delta), \tag{5}$$

while the derivative becomes[20]

$$\left\langle \xi_{n'}\left|\frac{\partial}{\partial\chi}\right|\xi_n\right\rangle=\begin{cases}0, & \text{for } n'=n\\[2ex] \dfrac{(-1)^{n'-n}}{(n'-n)\Delta}, & \text{for } n'\neq n.\end{cases} \tag{6}$$

As stated before, the Hermitian adjoints are simply obtained by bringing the operator from ket to bra, after which again a resolution of identity is inserted.

The products of the three-particle operators $j_z^\dagger j_z$ and $j_\pm^\dagger j_\pm$ occurring in H^{int} are treated as follows: Since $j_\pm$ and j_z are sums of one-particle terms we meet matrix elements of cross terms and quadratic terms. The cross terms factorize into one-particle terms and are computed as just explained. The diagonal terms in $j_z^\dagger j_z$ are of the form

$$\frac{\partial}{\partial\chi}\sin^2\chi\frac{\partial}{\partial\chi}=\sin\chi\frac{\partial^2}{\partial\chi^2}\sin\chi+\cos^2\chi + \left[\sin\chi\,\cos\chi,\frac{\partial}{\partial\chi}\right], \tag{7}$$

where we have rewritten the operator in terms that are Hermitian and can be efficiently computed. Substitution of the (truncated) resolution of identity leads to diagonal matrices representing $\sin\chi$, $\cos\chi$ and their product and non-diagonal matrices representing the differential operators. The same procedure is followed for the terms arising in $j_\pm^\dagger j_\pm$, where we write

$$\frac{\partial}{\partial\chi}\cos^2\chi\frac{\partial}{\partial\chi}=\cos\chi\frac{\partial^2}{\partial\chi^2}\cos\chi+\sin^2\chi - \left[\sin\chi\,\cos\chi,\frac{\partial}{\partial\chi}\right]. \tag{8}$$

In order to reduce the size of the Hamiltonian matrix, it is advantageous to adapt the DVR product functions $\xi_{n_A}(\chi_A)\xi_{n_B}(\chi_B)\xi_{n_C}(\chi_C)$ to the irreps of the group G_6 so that they transform in the same way as the functions $\Phi_k(\chi_A, \chi_B, \chi_C)$ in Eq. (I.9). The resulting expressions for the matrix elements of $H^{\rm int}$ are analogous to the numerator of Eq. (I.10), and for the Coriolis coupling matrix elements to Eqs. (B7), (B8), and (B9).

To determine the energy levels one can follow two different routes. The first route is to diagonalize $H=H^{\rm int}+H^{\rm rot}+H^{\rm Cor}$ directly in a basis of symmetry adapted DVR functions in χ_A, χ_B, χ_C, multiplied with the eigenfunctions $|JKM\rangle$ of $H^{\rm rot}$, for given J (and arbitrary M). The second route is to diagonalize first $H^{\rm int}$ in the symmetry adapted DVR basis, and then to use a (truncated) set of eigenvectors of $H^{\rm int}$, multiplied with the eigenfunctions $|JKM\rangle$ of $H^{\rm rot}$, to diagonalize $H^{\rm Cor}$. We followed both routes. We found that we need the lowest 60 eigenvectors of $H^{\rm int}$, i.e., 10 eigenvectors of each G_6 irrep, to obtain the relatively large Coriolis splittings of the lowest A_2^-, A_3^- and A_3^+, A_2^+ levels with $|k|=1$ and $|k|=2$ converged to within 1%, for $J=1$. With 25 eigenvectors of $H^{\rm int}$ for each G_6 irrep these splittings are converged to within 0.01%. The very small splittings of the ground A_1^+ level with $k=0$ and the lowest A_1^- level with $k=3$ which are due to the combined effect of Coriolis coupling and donor tunneling (see below) are converged already to within 1% with three eigenvectors of $H^{\rm int}$ for each G_6 irrep. The reason for this fast convergence is that for $J=1$ the matrix elements of $H^{\rm Cor}$ are only about 1% of the energy gaps between the different eigenvalues of $H^{\rm int}$. The second method has the advantages that it is computationally more efficient and gives explicitly the Coriolis coupling constants between the different eigenstates of $H^{\rm int}$, which are the parameters Q_J in the qualitative model of paper I.

In addition, we computed the donor tunneling splittings. Since a high quality *ab initio* potential surface including the donor tunneling coordinates is not available, we could not perform explicit six-dimensional calculations with the inclusion of these coordinates. So we were forced to combine our quantitative calculations of the pseudo-rotation with the model treatment for donor tunneling described in Secs. IV and V of paper I. For the parameters δ_1 and δ_2 in the donor tunneling matrix elements between the functions Φ_k and Φ_{-k} for $|k|=1$ and $|k|=2$ we introduce empirical values. The mixing between functions that carry different G_6 irreps k and $-k$ becomes allowed, because donor tunneling leads to the larger symmetry group G_{48} and the irreps k and $-k$ induce to the same irreps $T_g^{\pm}$ and $T_u^{\pm}$ of G_{48} (see paper I). Hence, we can no longer separate the Hamilton matrix for the total problem including the rotation functions $|JKM\rangle$ into blocks with different G_6 irrep labels $k-K$. Only the blocks with even values of $k-K$ separate from those with odd values. For the one-dimensional G_{48} irreps $A_{1g}^{\pm}, A_{2g}^{\pm}, A_{3g}^{\pm}, A_{1u}^{\pm}, A_{2u}^{\pm}, A_{3u}^{\pm}$ such donor tunneling coupling between the functions Φ_k and Φ_{-k} does not occur, and one can still use the $k-K$ labeling of the final states. We computed the levels for $J=0$, 1 and 2. Although semi-empirical, such quantitative calculations including donor tunneling are useful, because they yield the splittings induced by the combined effect of Coriolis coupling and donor tunneling, without having to resort to the (approximate) perturbation theory used in paper I.

B. Results

Before discussing our results, we make some comparisons with the three-dimensional calculations of the pseudo-rotation tunneling levels performed by Sabo *et al.*,[8] who based their work on the BGLK-potential,[15] and by Meijer *et al.*,[9] who used the DD-potential.[14,18] Sabo *et al.* applied a three-dimensional DVR method, with a quadrature and a basis which are different from ours, and Meijer *et al.* used a basis of harmonic oscillator functions. In both papers the Hamiltonian for the pseudo-rotation tunneling has the form of our operator $H^{\rm int}$, see Eq. (I.8), but without the terms containing the operators j_z and $j_{\pm}$. Also their effective rotational constants $\hbar^2/(2\Lambda)$ for the constrained monomer rotations, which they derived heuristically, were different from ours. Sabo *et al.* used the value 23.49 cm^{-1} for H_2O, Meijer's reduced mass corresponds to a value of 20.64 cm^{-1}, whereas we derived that this constant should be 21.39 cm^{-1}. Still, it is useful to know that our eigenvalues of $H^{\rm int}$ agree to within 0.1 cm^{-1} with those of Sabo *et al.*, and to within 0.2 cm^{-1} with those of Meijer , if we use their potentials and their values for the rotational constants and restrict $H^{\rm int}$ to the terms which they include. For the lowest six eigenvalues the agreement is even better, about 0.01 cm^{-1} with Sabo *et al.* and about 0.05 cm^{-1} with Meijer *et al.* As the methods and basis sets in the three calculations are different and have been independently programmed, this provides a check of the correctness of the programs and of the basis set and DVR grid convergence.

In Table I we list the pseudo-rotation tunneling levels for $J=0$, i.e., the eigenvalues of the complete operator $H^{\rm int}$ in Eq. (I.8). The first observation that can be made is that the contribution of the terms $\frac{1}{2}A(j_+^{\dagger}j_+ + j_-^{\dagger}j_-) + Cj_z^{\dagger}j_z$ in $H^{\rm int}$ is relatively small, but certainly not negligible. The differences with the energies calculated by Sabo *et al.*[8] with the BGLK-potential and by Meijer *et al.*[9] with the DD-potential are mainly due to the different values of the effective rotational constant $\hbar^2/(2\Lambda)$. The differences between the results from the two *ab initio* potentials are quite large. We observe, in particular, in Table I that the BGLK-potential gives substantially lower energies of the lowest four levels (six states), and that the order of some of the higher levels is reversed. In agreement with the previous calculations we find that the excitation frequencies for $(D_2O)_3$ are about half of those for $(H_2O)_3$.

All the calculations yield the result that the lowest six states—with $k=0,\pm1,\pm2,3$ (those with $k=\pm1$ and ±2 being degenerate)—are separated by a large energy gap from the higher levels. This, and the fact that the gaps between these lower levels nearly have the ratio 1:2:1, confirms that both Wales'[10] and our model for the pseudo-rotation tunneling levels with gaps of β_1, $2\beta_1$, β_1 (see Table II in paper I)

TABLE I. Pseudo-rotation tunneling levels for $J=0$ with the DD-potential (Refs. 14 and 18) and the BGLK-potential (Ref. 15), in cm^{-1}. In parentheses are the contributions of the term $\frac{1}{2}A(j_+^\dagger j_+ + j_-^\dagger j_-) + Cj_z^\dagger j_z$ in H^{int}. The energies are given relative to the zero point levels, which are 251.36, 281.75, 201.94, and 224.92 cm^{-1}, respectively.

		$(H_2O)_3$				$(D_2O)_3$	
G_6 irrep	k	DD-potential	BGLK-potential	G_6 irrep	k	DD-potential	BGLK-potential
A_1^+	0	0.00(0.84)	0.00(1.06)	A_1^+	0	0.00(1.25)	0.00(1.53)
A_2^-, A_3^-	±1	19.93(1.30)	13.97(1.39)	A_2^-, A_3^-	±1	7.68(1.54)	5.15(1.73)
A_3^+, A_2^+	±2	59.07(1.94)	44.15(1.94)	A_3^+, A_2^+	±2	25.18(2.08)	17.15(2.15)
A_1^-	3	81.23(1.87)	62.33(2.02)	A_1^-	3	36.62(2.34)	24.73(2.38)
A_1^-	3	161.01(3.17)	143.85(3.09)	A_1^-	3	96.15(3.25)	88.93(3.14)
A_1^+	0	165.34(2.01)	181.11(1.96)	A_3^+, A_2^+	±2	107.51(2.97)	98.27(3.03)
A_3^+, A_2^+	±2	172.02(2.24)	155.18(2.42)	A_2^-, A_3^-	±1	129.76(2.95)	117.77(2.91)
A_1^-	3	175.93(1.64)	180.45(1.51)	A_1^+	0	132.50(2.72)	130.07(2.77)
A_2^-, A_3^-	±1	209.19(2.75)	188.70(2.52)	A_1^-	3	143.24(1.62)	151.63(1.89)
A_1^+	0	229.07(1.61)	207.02(1.88)	A_1^+	0	155.04(1.92)	160.66(2.39)
A_2^-, A_3^-	±1	238.21(2.89)	237.04(3.02)	A_2^-, A_3^-	±1	165.38(3.38)	173.43(3.41)
A_3^+, A_2^+	±2	248.76(3.44)	237.75(3.21)	A_3^+, A_2^+	±2	166.95(2.98)	165.91(2.82)
A_1^-	3	288.49(2.45)	276.65(2.36)	A_1^+	0	191.44(4.45)	173.81(4.47)

is indeed valid. This holds for both potentials, for $(H_2O)_3$ as well as for $(D_2O)_3$, and it may be observed that the energy formula in Eq. (I.12) represents these levels even better if the overlap $S=\langle u|d\rangle$ in the denominator is not neglected.

Table II contains the Coriolis coupling constants, i.e., the matrix elements of the shift operators $j_\pm + j_\mp^\dagger$ in H^{Cor} between the eigenstates of H^{int}. The numbers in the first row are the matrix elements $\frac{1}{2}A|\langle\Phi_k|j_- + j_+^\dagger|\Phi_{k+1}\rangle|$ between the lowest six internal states which occur in our model, see Eq. (I.21). It is remarkable that the ratio of these numbers is nearly 1:2:1 for the matrix elements (0,1), (1,2), and (2,3), just as predicted by Eq. (I.21). Again, this holds for both potentials, although slightly better for $(H_2O)_3$ than for $(D_2O)_3$, which confirms that our model also gives the correct Coriolis coupling constants. The coupling constants with the higher levels, in the second and third rows of Table II, are comparable in size to those in the first row. Since there is a large energy gap between these higher states and the lowest six, the role of this coupling to the higher levels is less important than the coupling among the lower levels. But, as we will see in our quantitative calculations of the levels for $J>0$, it is certainly not negligible.

Tables III and IV contain the energy levels calculated for $(H_2O)_3$ and $(D_2O)_3$ for $J=1$ and 2, by direct or stepwise diagonalization of the complete Hamiltonian $H=H^{int}+H^{rot}+H^{Cor}$, see Sec. II A. It must be noted that the absolute accuracy of the energy levels is not better than 0.01 $cm^{-1}=300$ MHz, for the given potential—we used the DD-potential of Ref. 18 in this case. Still, we present these energies with many digits, because the Coriolis and donor tunneling splittings of the degenerate levels with given $|k|$ and $|K|$ are computed to much greater precision, and we wish to show these splittings.

In Table III we look in particular at the Coriolis splitting of the $|k|=1$ levels with $|K|=1$, which would have been fourfold degenerate without this splitting. As discussed in Sec. V and visualized in Fig. 2, both of paper I, they split into two levels with $k-K=0$ and a twofold degenerate level with $k-K=\pm 2$. According to the qualitative results in Table III of paper I, the splitting of the two levels with $k-K=0$ should have nearly the same size as the gap between the lowest of these levels and the level with $k-K=\pm 2$. In Table III we observe, however, that this is not the case. For $J=1$ the splittings of the levels with $k-K=0$ are

TABLE II. Coriolis coupling constants $\frac{1}{2}A|\langle k|j_- + j_+^\dagger|k+1\rangle|$, absolute values in cm^{-1}, between the lowest state of k-symmetry and the lowest three states of $(k+1)$-symmetry.

	DD-potential			BGLK-potential		
$(k,k+1)$	(0,1)	(1,2)	(2,3)	(0,1)	(1,2)	(2,3)
$(H_2O)_3$						
	0.155	0.316	0.154	0.119	0.260	0.141
	0.081	0.262	0.458	0.021	0.258	0.433
	0.313	0.141	0.318	0.335	0.150	0.289
$(D_2O)_3$						
	0.099	0.228	0.139	0.073	0.169	0.102
	0.003	0.245	0.428	0.061	0.245	0.400
	0.402	0.202	0.273	0.365	0.153	0.240

TABLE III. Pseudo-rotation tunneling levels including Coriolis coupling for $J=1$ (in MHz), relative to the ground level with $J=0$. These levels, calculated with the DD-potential (Refs. 14 and 18), are the levels that belong to the one-dimensional irreps of G_{48}. The donor tunneling energies that must be added to these levels for the g/u irreps are given in the last colum in terms of the parameter β_3; the parameter β_2 is neglected (see the text).

k	G_{48} irreps	K	$k-K$	$(H_2O)_3$	$(D_2O)_3$	g/u
0	A_{1g}^+/A_{1u}^+	±1	±1	9 860.867	8 730.129	$+\beta_3/-\beta_3$
		0	0	13 077.427	11 289.649	
±1	$A_{2g}^-, A_{3g}^-/A_{2u}^-, A_{3u}^-$	±1	±2	607 360.316	238 831.434	$-\beta_3/+\beta_3$
			0	607 541.190	239 052.602	
			0	607 550.338	239 065.288	
		0	±1	610 669.965	241 505.057	
±2	$A_{3g}^+, A_{2g}^+/A_{3u}^+, A_{2u}^+$	±1	3	1 780 569.876	763 493.962	$+\beta_3/-\beta_3$
			3	1 780 573.783	763 498.237	
			±1	1 780 861.122	763 832.118	
		0	±2	1 783 933.964	766 224.733	
3	A_{1g}^-/A_{1u}^-	±1	±2	2 445 123.019	1 106 514.123	$-\beta_3/+\beta_3$
		0	3	2 448 340.782	1 109 075.403	

only 9.1 and 12.7 MHz for $(H_2O)_3$ and $(D_2O)_3$, respectively, while the gaps with the $k-K=\pm2$ levels are 180.9 and 221.2 MHz. The same picture occurs for the splittings of the fourfold degenerate levels with $|k|=2$ and $|K|=1$, i.e., the splitting of the two levels with $k-K=3$ is much smaller than the gap between these levels and the twofold degenerate level with $k-K=\pm1$. We have analyzed why our qualitative model does not hold in this case, and we found that this is due to Coriolis coupling with the higher states. These higher states are not included in our simple model, but by looking at our theoretical results we can perfectly understand what happens. As we have seen in the second and third rows of Table II, there are substantial coupling matrix elements between these higher levels and the states under discussion. For the levels with $k-K=\pm2$ and ±1 this leads to a normal type of second order Coriolis perturbation. The splitting of the levels with $k-K=0$ follows from degenerate second order perturbation theory, however, which mixes the degenerate states $|1,1\rangle$ and $|-1,-1\rangle$, with equal weights but with complex coefficients. Since the phases of the (complex) Coriolis coupling constants differ for the different perturbing states, there is a strong (destructive) interference of the resulting Coriolis splitting of the levels with $k-K=0$. By consequence, the splitting of these levels is relatively small. Equivalently, for $k-K=3$, the functions $|2,-1\rangle$ and $|-2,1\rangle$ are coupled to the different perturbing states with different phases, and the splitting of these levels is also small.

For a proper understanding of the results in Tables III and IV, we first remind the reader that every state calculated without donor tunneling (and, therefore, adapted to the group G_6) splits into a quartet by donor tunneling (and adaptation to G_{48}). Two of the levels in each quartet belong to the one-dimensional irreps $A_{ig}^{\pm}$ and $A_{iu}^{\pm}$ of G_{48}, with $i=1$, 2, or 3, and the other two levels belong to the irreps $T_u^{\pm}$ and $T_g^{\pm}$. Remember that the subscripts g and u in the irrep labels are related with the parity of the states under donor tunneling, while the $\pm$ superscripts refer to their parity under inversion, E^*. The (first order) donor tunneling splittings of the levels in these quartets are given for $J=0$ in Table II of paper I, in terms of the parameters β_2 and β_3. In Tables III and IV we list the corresponding levels for $J>0$; Table III

TABLE IV. Pseudo-rotation tunneling levels of $(H_2O)_3$ including Coriolis coupling for $J=1$ and 2, (in MHz), relative to the ground level with $J=0$. These levels, calculated with the DD-potential (Refs. 14 and 18) and the parameter values $2\delta_1=-2\delta_2=289$ MHz, are the levels that belong to the three-dimensional irreps of G_{48}. The donor tunneling energies that must be added to these levels for the T_u/T_g irreps are given in the last colum in terms of the parameter β_3; the parameter β_2 is neglected (see the text). The donor tunneling splittings caused by the interaction between states of the same symmetry are included in the numerical values.

$\|k\|$	G_{48} irreps	$\|K\|$	$J=1$	$J=2$	T_u/T_g
0	T_u^+/T_g^+	1	9 860.849	36 015.631	$+\frac{1}{3}\beta_3/-\frac{1}{3}\beta_3$
		1	9 860.885	36 015.739	
		0	13 077.427	39 232.280	
1	T_u^-/T_g^-	1	607 280.291	633 434.155	$-\frac{1}{3}\beta_3/+\frac{1}{3}\beta_3$
		1	607 282.417	633 440.536	
		1	607 621.205	633 770.166	
		1	607 628.246	633 791.285	
		0	610 525.505	636 681.584	
		0	610 814.425	636 970.344	
2	T_u^+/T_g^+	1	1 780 510.364	1 806 664.740	$+\frac{1}{3}\beta_3/-\frac{1}{3}\beta_3$
		1	1 780 513.702	1 806 674.756	
		1	1 780 920.629	1 807 077.627	
		1	1 780 921.207	1 807 079.359	
		0	1 783 789.509	1 809 947.249	
		0	1 784 078.420	1 810 235.983	
3	T_u^-/T_g^-	1	2 445 122.997	2 471 281.233	$-\frac{1}{3}\beta_3/+\frac{1}{3}\beta_3$
		1	2 445 123.040	2 471 281.361	
		0	2 448 340.782	2 474 499.039	

TABLE V. Observed and calculated transitions, frequencies in cm^{-1}.

	Experiment			Calculated frequencies			
	Freq.	Type	Assignment[a]	Ref. 7	Ref. 8	DD-potential	BGLK-potential
$(H_2O)_3$							
	87.1	*c*	$k=3\leftarrow 0$	88.6	69.6	81.2	62.3
$(D_2O)_3$							
	41.1	*c*	$k=3\leftarrow 0$	40.9	24.0	36.6	24.7
	98.1	*a*	$k=\pm 2(\text{upper})\leftarrow 0$	97.8	96.9	107.5	98.3
	89.6	*c*	$k=\pm 2(\text{upper})\leftarrow \pm 1$	91.4	91.9	99.8	93.1
	82.5	*a*	$k=3(\text{upper})\leftarrow \pm 1$?	71.0	82.5	88.5	83.8

[a]The assignment proposed by Klopper and Schütz (Ref. 7), is confirmed (see the text); ''upper'' denotes those levels that do not belong to the lowest states with $k=0,\pm 1,\pm 2,3$.

contains the results for the one-dimensional irreps of G_{48} and Table IV the results for the irreps $T_g^{\pm}$ and $T_u^{\pm}$. Combining these results yields the quartets for $J>0$. For the states that belong to the $T_g^{\pm}$ and $T_u^{\pm}$ irreps, i.e., the levels in Table IV, there is an additional splitting, because two states of the same symmetry occur in every level that belongs to the G_6 irreps with labels $k=\pm 1$ or $k=\pm 2$. The interaction between these two states can be simply expressed in terms of the matrix elements δ_1 and δ_2, see Eqs. (I.17) and (I.18). The additional splittings that result for $J=0$ are included in Table II of paper I. For $J=1$ and $J=2$ they are contained in the numerical values in Table IV. The levels in this table were obtained by the inclusion of the donor tunneling matrix elements $\exp(2\pi i/3)\delta_1$ and $\exp(2\pi i/3)\delta_2$ that couple the internal states with $k=\pm 1$ and those with $k=\pm 2$, with the empirical values $2\delta_1=-2\delta_2=289$ MHz. These values were extracted from the spectrum of $(H_2O)_3$ measured by Liu *et al.*,[2,3] in a way which is described in Sec. III. For $J>0$, there is a complex interplay between Coriolis coupling and donor tunneling, as discussed in Sec. V of paper I. It is the combined effect of these two mechanisms which is visible in Table IV.

All degeneracies are now lifted (see Fig. 3 in paper I) and we observe three different types of splittings in Table IV. The splitting of the $K=0$ levels with $|k|=1$ and $|k|=2$ is caused merely by donor tunneling. It is J-independent and nearly equal to the donor tunneling splittings $2\delta_1$ and $2\delta_2$ of the corresponding levels for $J=0$. The splitting of the fourfold degenerate $|K|=1$ levels with $|k|=1$ is less regular, because the (second order) Coriolis coupling mixes the functions $|1,1\rangle$ and $|-1,-1\rangle$, while the (first order) donor tunneling mixes $|1,1\rangle$ with $|-1,1\rangle$, and $|1,-1\rangle$ with $|-1,-1\rangle$. Since the strength of these two effects is nearly equal, cf. Eq. (I.25), this yields an irregular J-dependent splitting of these levels and, similarly, of the fourfold degenerate $|K|=1$ levels with $|k|=2$. Finally, we observe in Table IV that also the $|K|=1$ levels with $k=0$ are now split, as well as those with $k=3$. This is the very small splitting discussed at the end of Sec. V in paper I, which is caused by donor tunneling through the Coriolis mixing with the $|k|=1$ and $|k|=2$ states. The splittings of ± 0.018 MHz for $k=0$ and ± 0.021 MHz for $k=3$, relative to the corresponding levels with $J=1$ in Table III, are very close to the values that we predicted by perturbation theory. Moreover, we can conclude by comparing the results for $J=1$ and $J=2$ in Table IV that these splittings are indeed proportional to $J(J+1)$. So, we may conclude that our qualitative model is valid also for these small splittings. We will use these observations in our interpretation of the measured spectra in Sec. III.

III. EXPERIMENTAL SPECTRUM, INTERPRETATION

A. Experiment

In this section we present new experimental data obtained with the Berkeley tunable FIR laser spectrometer. This spectrometer and its recent improvements have been described in detail elsewhere.[21,22] Briefly, tunable far-ir radiation is generated by mixing an optically pumped far-ir laser with continuously tunable microwave (mw) radiation in a Schottky barrier diode. The resulting tunable sidebands $(=\nu_{\text{far-ir}}\pm\nu_{\text{mw}})$ are directed into a vacuum chamber wherein they are multipassed 22 times nearly orthogonal to a pulsed planar supersonic jet containing clusters of interest. The direct absorption signal is detected by a liquid helium cooled stressed Ga:Ge photoconductor. Jet-cooled water clusters were produced and cooled to ≈ 5 K by bubbling argon through room-temperature water and expanding the saturated gas through either a pulsed or cw slit nozzle of the same dimensions, 101.6 mm by 0.100 mm. In the former case, a double modulation detection scheme was employed, wherein a digital lock-in amplifier (Stanford Research Systems, SRS 830) recovered the frequency-modulated laser sideband signals at a time constant of 100 μs and twice the reference frequency ($2f=100$ kHz). The output of the lock-in was then fed in two boxcars (SRS 250) for gated integration and averaging at the pulse repetition rate (40–60 Hz); one samples the peak of the transient absorption, and the other the background. For the cw nozzle, only a lock-in operating at a longer time constant (300 ms) was required for the signal detection. A significant increase in the cluster number density obtained with the pulsed slit nozzle has permitted an improvement in the signal-to-noise ratio up to an order of magnitude compared with that obtained using the cw jet.

The far-infrared bands observed thus far for $(H_2O)_3$ and $(D_2O)_3$ are collected in Table V. As inferred from combination differences, the *c*-type transition at 41.1 cm^{-1} (Ref. 5)

and the a-type transition at 98.1 cm^{-1} (Refs. 2 and 3) must have a common origin, which is probably the ground state of $(D_2O)_3$. Also for the a-type transition at 98.1 cm^{-1} (Refs. 2 and 3) and the c-type transition at 89.6 cm^{-1} (Ref. 1) we have recently found combination differences, which prove that these transitions share their upper levels.

It was observed that most rovibrational transitions are split into quartets. From the relative intensities of the lines in these quartets for $(D_2O)_3$ and the observation that for $(H_2O)_3$ one line is missing for the levels with K_c values not equal to a multiple of 3, it was concluded by Liu *et al.*[2] that the molecular symmetry group of the water trimer is G_{48}, and that the equal spacing of the lines in each quartet is caused by donor tunneling. This conclusion is based on the nuclear spin statistical weights associated with the permutation-inversion group G_{48}, see Table II in paper I. According to Liu *et al.*, each rovibrational energy level is split by donor tunneling into a quartet of levels which carry different G_{48} irreps. In their notation these are the irreps $A_i^{\pm}, F_A^{\pm}, F_B^{\pm}, B_i^{\pm}$ with $i=1$, 2, or 3. In our notation the A_1, A_2, A_3 irreps are denoted as A_{1g}, A_{2g}, A_{3g}, the B_1, B_2, B_3, irreps as A_{1u}, A_{2u}, A_{3u}, and the F_A and F_B irreps as T_u and T_g, respectively. Since transitions are allowed only within the same irrep, except for its $\pm$ parity, the quartet splitting of the levels gives rise to quartets of peaks in the spectra. For $(H_2O)_3$ the quartet line spacing is 289 MHz,[2] for $(D_2O)_3$ it is about 1.5 MHz in the band at 41.1 cm^{-1} (Ref. 5) and about 5 MHz in the band at 98.1 cm^{-1}.[2,3] Actually, as one observes in Table II of paper I, the situation is more complicated for the degenerate levels with $k=\pm 1$ and ± 2.

In Fig. 1 and Table VI we show our new experimental data for the $(H_2O)_3$ band at 87.1 cm^{-1}, which demonstrate that those lines in the quartets which correspond to the transitions within the irreps T_u and T_g are further split into doublets. This splitting occurs only for P and R type transitions, however, not for the Q branches. Moreover, it is not constant, but increases with the rotational quantum number J.

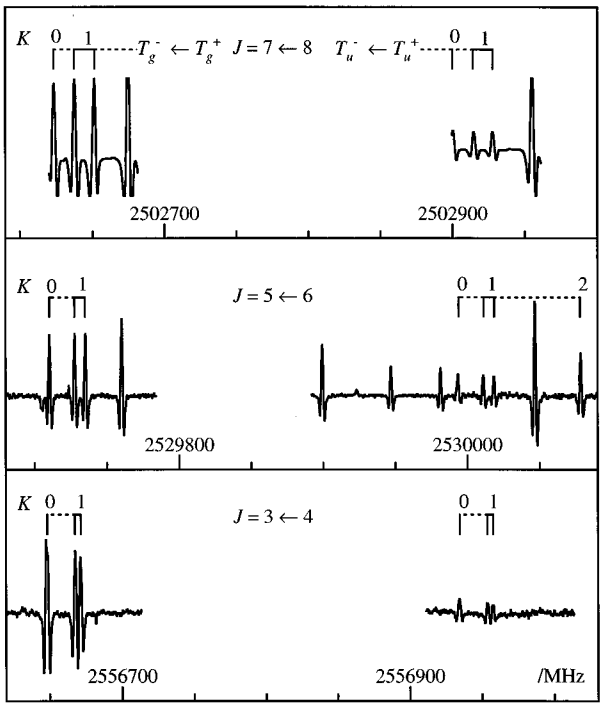

FIG. 1. The far-infrared VRT spectra of the $P(4)$, $P(6)$, and $P(8)$ transitions of the $\Delta K=0$ band of $(H_2O)_3$ at 87.1 cm^{-1}. Note that for the T_g and T_u symmetry components of the donor tunneling quartet, the transitions between $|K|=1$ substates exhibit extra doubling which increases with J, as a result of donor tunneling induced by Coriolis mixing (as explained in the text). The characteristic 289 MHz quartet line spacing is evident in the transitions between the $K=0$ substates of the same J. The intensity ratio between the T_g and T_u states of the same J and K approximates the predicted 9:3 nuclear spin statistical weights. Note the better signal/noise ratio even for the $P(8)$ transition due to the use of a pulsed planar supersonic jet (Ref. 22), instead of a cw one used for the $P(4)$ and $P(6)$ transitions.

B. Interpretation and discussion

Before we discuss the observations in the light of our theory and quantitative results, let us consider the selection rules. As shown in Appendix B of paper I, these can be derived from symmetry considerations. The overall dipole function in Eq. (B3) has A_1^- symmetry in the group G_6, i.e., it carries the irrep with label $k=3$. This gives the selection rule that transitions are allowed only when the initial and final states differ by 3 in their total quantum number $k-K$. By looking at the symmetry of the ''internal'' dipole function in Eq. (B1), we find more specific selection rules. The z component μ_0^{BF} also carries the A_1^- irrep and, hence, the internal states involved in a parallel transition with $\Delta K \equiv \Delta K_c = 0$ must satisfy the condition $\Delta k = \pm 3$. Parallel (c-type) transitions occur for $k=0 \leftrightarrow k'=3$ and for $|k|=1 \leftrightarrow |k'|=2$. The ± 1 components of $\boldsymbol{\mu}^{BF}$ carry the irreps A_3^+ and A_2^+ with labels $k=\pm 2$, so that perpendicular (a-type) transitions with $\Delta K=\pm 1$ and $\Delta k=\pm 2$ are allowed only between internal states with $k=0 \leftrightarrow |k'|=2$ and with $|k|=1 \leftrightarrow k'=3$.

An assignment of the observed bands (see Table V) was proposed by Klopper and Schütz.[7] The energy levels which they computed from their 2-dimensional model for the pseudo-rotations agree well with the observed frequencies, but it should be noted that the parameters F and R in their model were fitted to these frequencies. It is noteworthy that the BGLK-potential, on which they based their calculations, gives frequencies for the transitions among the lower levels which are substantially too low when used in more accurate three-dimensional calculations.[8] In our calculations of the three-dimensional pseudo-rotation levels with this BGLK-potential we also obtain frequencies for the transitions among the lower levels which are much too low. The corresponding transition frequencies that we compute from the DD-potential agree much better with the measured values. Actually, the agreement with experiment for these frequencies in our *ab initio* computations with the latter potential is so good that this calculation confirms the assignment of the c-type bands in $(H_2O)_3$ and $(D_2O)_3$ at 87.1 and 41.1 cm^{-1},

TABLE VI. Splittings (in MHz) found in the c-type ($\Delta K_c=0$) band at 87.1 cm^{-1} for $(H_2O)_3$. These doublets are observed only for the P and R branch transitions between the $K_c=1$ levels of the T_u and T_g states. The splittings in the column ''calc.'' are obtained from the fit with $2cJ^2$ and $2c(J+1)^2$ for the P and R branch transitions, respectively, and $c=0.106$ MHz. There is no splitting evident in the Q branch region, see Fig. 2 of Ref. 2.

Assignment	$T_g^- \leftarrow T_g^+$		$T_u^- \leftarrow T_u^+$		
$K_c=1$	Frequencies	Splittings	Frequencies	Splittings	Calc.
$P(8)$	2 502 637.5	13.8	2 502 914.7	13.0	13.5
	2 502 651.3		2 502 927.7		
$P(6)$	2 529 727.7	7.4	2 530 011.3	7.4	7.6
	2 529 735.1		2 530 018.7		
$P(5)$	2 543 213.5	5.2	2 543 499.3	5.0	5.3
	2 543 218.7		2 543 504.3		
$P(4)$	2 556 667.7	3.6	2 556 954.1	3.6	3.5
	2 556 671.3		2 556 957.7		
$P(3)$	2 570 081.7	1.9	2 570 368.7	1.9	1.9
	2 570 083.6		2 570 370.6		
$R(2)$	2 649 712.1	2.0	2 649 999.9	2.2	1.9
	2 649 714.1		2 650 002.1		
$R(3)$	2 662 831.3	3.4	2 663 117.7	4.2	3.5
	2 662 834.7		2 663 121.9		
$R(4)$	2 675 905.3	5.3	2 676 190.3	5.3	5.3
	2 675 910.6		2 676 195.6		
$R(5)$	2 688 932.1	9.2	2 689 215.6	7.3	7.6
	2 688 941.3		2 689 222.9		

respectively, to the transition from the $k=0$ ground state to the lowest $k=3$ level.

Given this good agreement with experiment for the transitions among the lower levels with the DD-potential, and the considerably worse agreement with the BGLK-potential, it is puzzling that the latter potential gives much better frequencies for the transitions to the upper levels. The assignment of the transitions at 98.1 and 89.6 cm^{-1} in $(D_2O)_3$ can be given reliably now. From the observed combination differences with the band at 41.1 cm^{-1} it is clear that the transition at 98.1 cm^{-1} must leave from the $k=0$ ground state. And from the combination differences which establish that the latter (a-type) transition shares its upper ($|k|=2$) levels with the transition at 89.6 cm^{-1} it follows that the latter (c-type) transition must leave from the lowest $|k|=1$ level. The frequency difference of $98.1-89.6=8.5$ cm^{-1} agrees well with the energy gap of 7.7 cm^{-1} between the lowest $|k|=1$ level and the ground $k=0$ level that we calculate for $(D_2O)_3$ with the DD-potential. So it is certain that the band at 89.6 cm^{-1}, first observed by Pugliano and Saykally,[1] is indeed a hot band[2] starting from the lowest level with $|k|=1$. The strong perturbations found in this band agree with the result from our calculations that the $|k|=1$ and $|k|=2$ levels are strongly perturbed. Also for the band at 82.5 cm^{-1} one should observe combination differences with the band at 89.6 cm^{-1}, if the assignment of Table V is correct and these bands share their initial levels. The finding that the BGLK-potential gives much better frequencies for the transitions to the upper levels than the DD-potential seems to indicate that it is more accurate in the higher energy region, whereas the latter is more accurate at lower energies.

Next we discuss the observed splitting of each rovibrational line into a quartet, with line spacing 289 MHz for the $k=3\leftarrow 0$ transition at 87.1 cm^{-1} in $(H_2O)_3$ (Refs. 2 and 3) and about 1.5 MHz for the corresponding band at 41.1 cm^{-1} in $(D_2O)_3$.[5] These splittings are caused by donor tunneling; they can be interpreted with the results in Table II of paper I for $J=0$ and those in Tables III and IV of the present paper for $J>0$. According to the G_{48} selection rules, the transitions that lead to the observed quartets are $A_{1g}^- \leftarrow A_{1g}^+$, $T_u^- \leftarrow T_u^+$, $T_g^- \leftarrow T_g^+$, and $A_{1u}^- \leftarrow A_{1u}^+$. From the levels with $k=0$ and $k=3$ in Table II of paper I one can read that only the parameter β_3 of Wales' donor tunneling model[10] is reflected in these quartet line spacings; the shifts in the energy levels which are proportional to the other parameter (β_2) are the same for the upper and lower levels in each allowed transition. By subtraction of the energies in Table II of paper I, or those in Tables III and IV of the present paper, it is found that the spacings between the four peaks in each quartet are the same; they are all equal to $|(4/3)\beta_3|$. From the observed intensity ratios,[2] in relation with the nuclear spin statistical weights, it follows that the transitions in each quartet of the band at 87.1 cm^{-1} in $(H_2O)_3$ are ordered such that $A_{1g}^- \leftarrow A_{1g}^+$ is to the blue of $T_u^- \leftarrow T_u^+$, etc., with a spacing of 289 MHz. So we may infer from these line spacings and the order of the lines that $(4/3)\beta_3=-289$ MHz for the lowest levels with $k=0$ and $k=3$ in $(H_2O)_3$. For the corresponding $k=3\leftarrow 0$ transition at 41.1 cm^{-1} in $(D_2O)_3$ the relative intensities of the quartet lines,[5] in relation to the nuclear spin statistical weights, show that the order of the lines is the same as in the band at 87.1 cm^{-1} in $(H_2O)_3$. And, since the line spacing of the quartets in the band at 41.1 cm^{-1} is about 1.5 MHz, it follows that $(4/3)\beta_3=-1.5$ MHz for $(D_2O)_3$. Of course, we have assumed here that donor tunneling can be described by Wales' model or by a similar model, and that β_3 adopts the same values for the $k=0$ ground state and the $k=3$ excited state.

More generally, it follows from the group theoretical derivation of Eq. (I.16), that a donor tunneling pathway which involves inversion E^*, such as the mechanism associated with the operation $(12)^*$ which gives the coupling matrix element β_3, shifts the upper and lower levels of the same symmetry but opposite parity ($\pm$) in the opposite direction. The effects of such a mechanism are therefore directly visible in the observed $k=3\leftarrow 0$ transition frequencies. A donor tunneling pathway without inversion E^*, such as the mechanism associated with the permutation $(ACB)(154263)$ which gives the matrix element β_2, gives a parallel shift of the upper and lower levels in each transition, which is not reflected in the $k=3\leftarrow 0$ transition frequencies. For transitions involving the $|k|=1$ and $|k|=2$ levels the situation is more complex (see Sec. II B).

Finally we discuss the very small J-dependent doublet splittings which we observe for $(H_2O)_3$ in the c-type band at 87.1 cm^{-1}, see Table VI. Remember that the P and R branch transitions are split, while no splitting is observed for the Q branch,[2] and that this doublet splitting occurs only for the $T_u^- \leftarrow T_u^+$ and $T_g^- \leftarrow T_g^+$ transitions within each donor tunneling quartet. With the theoretical and computational results of paper I and Sec. II B, we can completely explain these ob-

servations. The c-type band at 87.1 cm^{-1} in $(H_2O)_3$ was already assigned to the transition from the $k=0$ ground state to the lowest excited $k=3$ level. This assignment was based on the agreement between the calculated and measured transition frequencies, but it is strengthened by the observation that a different assignment of this parallel band, namely to a $|k|=2\leftarrow 1$ (hot band) transition, is excluded for several reasons. We derived in paper I and computed in Sec. II B that the levels with $|k|=1$ and $|k|=2$ have Coriolis splittings of the same order of magnitude as the donor tunneling splittings and are strongly perturbed by the combination of these two effects. Also the relative intensities of the transitions between the donor tunneling substates of the levels with $|k|=1$ and $|k|=2$ are not so simple as those of the peaks in the quartets in the band at 87.1 cm^{-1}. Both the frequencies and the intensities in their spectrum are much more regular and the Coriolis perturbations are very small, which confirms the assignment of this band to the $k=3\leftarrow 0$ transition.

It follows from the theory in paper I and is confirmed by the quantitative results in Table IV that the $|K|=1$ levels with $k=0$ and $k=3$ are split (for the irreps T_g and T_u) into doublets by the combination of Coriolis coupling and donor tunneling. For the ground level with $k=0$ the splitting is approximately $2|Q_J|^2\delta_1/(E_1-E_0)^2$ and for the excited level with $k=3$ it is $2|Q_J|^2\delta_2/(E_3-E_2)^2$. With the use of Eqs. (I.21) and (I.24) for the Coriolis coupling constants Q_J between the states Φ_0 and Φ_1 and between the states Φ_2 and Φ_3, it follows that these splittings can be written as $cJ(J+1)$ and $c'J'(J'+1)$, with

$$c=\frac{1}{2}A^2|\langle\Phi_0|j_-+j_+^\dagger|\Phi_1\rangle|^2\delta_1/(E_1-E_0)^2,$$

$$c'=\frac{1}{2}A^2|\langle\Phi_2|j_-+j_+^\dagger|\Phi_3\rangle|^2\delta_2/(E_3-E_2)^2, \tag{9}$$

for the initial and final state, respectively. The energy gaps E_1-E_0 and E_3-E_2 in Table I and the (0,1) and (2,3) Coriolis coupling constants in the first row of Table II are nearly equal. Hence, if the donor tunneling matrix elements δ_1 and δ_2 given by Eqs. (I.17) and (I.18) are nearly equal too, it follows that the proportionality constants c and c' are nearly the same. Since $\delta_1=(2/3)(2\beta_2-\beta_3)$ and $\delta_2=(2/3)\times(2\beta_2+\beta_3)$ this is the case if β_2 is much larger (in absolute value) than β_3, as assumed by Wales.[10] If, on the other hand, β_3 is much larger than β_2, it follows that c and c' have nearly the same size but opposite sign. More generally, it follows from the same argument as used earlier in this discussion for the quartet splitting of the $k=3\leftarrow 0$ transitions in $(H_2O)_3$ and $(D_2O)_3$ that δ_1 and δ_2 have opposite sign if they are dominated by donor tunneling along a path that involves inversion, E^*, and the same sign if donor tunneling does not involve inversion. This is a consequence of the fact that δ_1 refers to the $|k|=1$ states with odd parity $(-)$, and δ_2 to the $|k|=2$ states with even parity $(+)$.

We will now consider the two cases $c'\approx c$ or $c'\approx -c$, which split each doublet with $k=0$ and the corresponding doublet with $k=3$ in the same or in opposite direction. The dipole matrix elements for $J'\leftarrow J$ transitions in this manifold are dominated by the main components of the wave functions involved in these transitions and by the parallel $(\kappa=0)$ component of the dipole operator in Eq. (B3)

$$\langle 3,\pm 1|\mu_m^{\mathrm{SF}}|0,\pm 1\rangle=\langle 3|\mu_0^{\mathrm{BF}}|\,0\rangle\langle\pm 1|D_{m0}^{(1)*}|\pm 1\rangle, \tag{10}$$

with the rotational matrix elements given in terms of $3j$-symbols by

$$\begin{aligned}\langle K|D_{m0}^{(1)*}|K\rangle&\equiv\langle J'KM'|D_{m0}^{(1)*}|JKM\rangle\\&=(-1)^{K-M'}[(2J'+1)(2J+1)]^{1/2}\\&\quad\times\begin{pmatrix}J' & 1 & J\\ -K & 0 & K\end{pmatrix}\begin{pmatrix}J' & 1 & J\\ -M' & m & M\end{pmatrix}.\end{aligned} \tag{11}$$

For P and R branch transitions with $J'=J\pm 1$ the two relevant dipole matrix elements with $K=1$ and $K=-1$ are equal. Taking the appropriate wave function combinations derived in Sec. V of paper I, we find that only two of the four possible transitions between the components of the initial and final doublet are allowed, with equal intensities. If δ_1 and δ_2 have the same sign, these are the transition from the lower level in the ground state $k=0$ doublet to the lower $k=3$ doublet level, and the transition from the upper ground state level to the upper excited level. The frequencies of these two transitions differ by $cJ(J+1)-c'J'(J'+1)$. For a P type transition with $J'=J-1$ and $c'\approx c$ each pair of peaks is split by $cJ(J+1)-c'J(J-1)\approx 2cJ$. If, on the other hand, the signs of δ_1 and δ_2 differ and $c'\approx -c$, the allowed transitions are from the lower level of the ground state doublet to the upper excited level and from the upper ground state level to the lower excited level, and the splitting of a P type transition is $cJ(J+1)-c'J(J-1)\approx 2cJ^2$. The P branch splittings listed in Table VI show a very clear quadratic dependence on J, hence it follows that $c'\approx -c$, i.e., that δ_1 and δ_2 must be nearly equal with opposite signs, and that β_2 must be negligible relative to β_3. A fit of the splittings with $2cJ^2$ gives a proportionality constant $2c$ of 0.21 MHz. Analogously, we derive for the case with $\delta_1\approx-\delta_2$ and $c'\approx -c$ that the R branch transitions with $J'=J+1$ are split by $2c(J+1)^2$. Also this agrees very well with the results in Table VI. The proportionality constant is the same as for the P band, as it should be. Its value, $c=0.106$ MHz, may be compared with the result that we can obtain from Eq. (9), as well as from the splitting of the $|K|=1$ levels with $k=0$ in Table IV. The relevant (0,1) and (2,3) Coriolis coupling constants are given in the first row of Table II and the energy gaps can be read from Table I. With the assumption that β_2 is indeed negligible relative to β_3, we find that $2\delta_1=-2\delta_2=-(4/3)\beta_3$. If we then extract the value $(4/3)\beta_3=-289$ MHz from the measured line spacing in the quartets of the $k=3\leftarrow 0$ transition at 87.1 cm^{-1} in Fig. 1, we find from Eq. (9) that $c=0.0175$ MHz with the DD-potential and 0.0210 MHz with the BGLK-potential. From the splitting of the $|K|=1$ levels with $k=0$ in Table IV we find that $c=0.018$ MHz, with the DD-potential. The fact that this value is about five times smaller than the experimental

value is probably caused by the use of the simplified model for donor tunneling and by the assumption that the first order donor tunneling splittings of the levels with $k=0$ and $k=3$ and the higher order coupling effects of these levels with the $|k|=1$ and $|k|=2$ states can all be described by a single donor tunneling parameter $(4/3)\beta_3$.

No splittings have been observed[2] in the Q band. This is also consistent with our interpretation, because $J'=J$ in this case, and the dipole matrix elements in Eqs. (10) and (11) have opposite signs for K and $-K$. Only the transitions from the upper level of each $k=0$ doublet to the upper level of the doublet with $k=3$, and from the lower level to the lower level, are then allowed. Since $c'\approx -c$ and the splittings of these doublets are nearly equal for $J'=J$, there should be no splittings in the Q band region of the spectrum, as observed. If, on the contrary, it would have been true that $c'\approx c$, the Q band would have been split by an amount $2cJ(J+1)$.

This pattern, a splitting of the P band proportional to J^2, a splitting of the R band proportional to $(J+1)^2$, and no splitting of the Q band, should be recognized by spectroscopists as the effect of asymmetry doubling in a nearly symmetric rotor, with ''axis switching.''[23] The water trimer is an oblate symmetric top; axis switching would imply that it is slightly asymmetric with nearly equal rotational constants A and B. The condition $A>B$ defines the principal a and b axes of the trimer, which would then refer to the x and y axes in the ground state and to the reversed situation in the excited state. In our treatment we have not imposed the asymmetry of the rotor, however, because we have assumed that the (vibrationally averaged) rotational constants A and B are equal. Instead, we have looked more in detail at the internal motions in the water trimer and investigated the effects of Coriolis coupling and donor tunneling. We found, among other things, that the combined effect of these two phenomena leads to a small doublet splitting of the ground and excited state, in the same or in opposite direction. If it is in opposite direction, it becomes manifest in the spectrum as ''axis switching.'' Thus we have identified the origin of the observed ''asymmetry doubling'' with axis switching, and we could ''read'' from the spectrum that the dominant donor tunneling pathway must involve inversion, E^*.

This explanation of the very small J-dependent splittings gives yet another confirmation that the band at 87.1 cm^{-1} in $(H_2O)_3$ is correctly assigned to the $k=3\leftarrow 0$ transition. Moreover, it allows us to conclude from the measured far-infrared spectrum that the donor tunneling pathway must involve inversion (E^*), in contrast with the *ab initio* calculations of Wales.[10]

An independent determination of the relative importance of the donor tunneling matrix elements β_2 and β_3 can be obtained from the relative intensities of the peaks in the quartets of the band at 98.1 cm^{-1} in $(D_2O)_3$. This is an a-type transition from the $k=0$ ground level to an upper level with $|k|=2$. We consider in particular the $K_c=0\leftarrow 1$ subband. The observed quartet intensity pattern is considerably different from the 70:108:54:8 ratio which corresponds to the nuclear spin statistical weights in the ground $K_c=1$ and $K_c=2$ states of $(D_2O)_3$, and which was observed for the

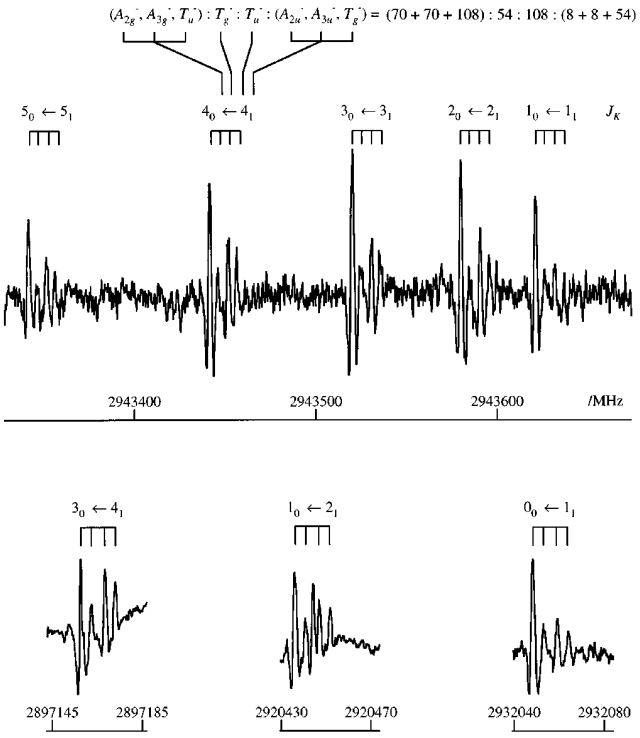

FIG. 2. The irregular donor tunneling quartet patterns observed for the $|K|=0\leftarrow 1$ subband of the $(D_2O)_3$ $k=\pm 2$ (upper) $\leftarrow 0$ transition (a-type) at 98.1 cm^{-1}. The intensity ratios are consistent with the donor tunneling splitting pattern obtained when β_2 is negligible and β_3' for the upper state is considerably larger than β_3 for the ground state. According to the G_{48} selection rules, $(k-K)=\pm 2$ (upper) $\leftarrow \pm 1$ correlates to VRT transitions between the following symmetry species: $A_{2g}^+\leftarrow A_{2g}^-(\beta_3' - \beta_3,70)$, $A_{3g}^+\leftarrow A_{3g}^-(\beta_3'-\beta_3,70)$, $T_u^+\leftarrow T_u^-(\beta_3'-\beta_3/3,108)$, $T_g^+\leftarrow T_g^-(\beta_3'/3+\beta_3/3, 54)$, $T_u^+\leftarrow T_u^-(-\beta_3'/3-\beta_3/3,108)$, $A_{2u}^+\leftarrow A_{2u}^-(-\beta_3'+\beta_3,8)$, $A_{3u}^+\leftarrow A_{3u}^-(-\beta_3'+\beta_3,8)$, $T_g^+\leftarrow T_g^-(-\beta_3'+\beta_3/3,54)$, with their donor tunneling splittings and spin weights (for the D_2O trimer) given in parentheses. Since the splittings $(2|\beta_3|/3)$ of the outermost peaks in the quartets are too small to be observed, the overall spin weight ratios are 248 $(=70+70+108)$:54:108:70$(=8+8+54)$ corresponding to the VRT states of $\{A_{2g}^-\oplus A_{3g}^-\oplus T_u^-\}$:$T_g^-$:T_u^- :$\{A_{2u}^-\oplus A_{3u}^-\oplus T_g^-\}$ symmetry, respectively. Note that the calculated pattern predicts slightly uneven line spacings: the separation between the central lines of weights 54 and 108 is larger by about $5|\beta_3|/3$ than the spacings between these lines and the two outer lines. Upon careful examination of the quartets in this figure this is indeed observed. The central peak in the $P(2)$ multiplet is not part of the trimer signal.

$K_c=2\leftarrow 2$ subband of the $k=3\leftarrow 0$ transition at 41.1 cm^{-1}. Instead, this ratio is more like 8:2:4:3. We can completely explain this observation on the basis of our theoretical results, and we will show now that this leads to an interesting conclusion.

The $|K|=0\leftarrow 1$ subband of the $|k|=2\leftarrow 0$ transition at 98.1 cm^{-1} has the overall G_6 symmetry designation $(k-K)=\pm 2\leftarrow \pm 1$ or $\{A_3^+,A_2^+\}\leftarrow\{A_2^-,A_3^-\}$. Each of the G_6 adapted internal states splits into a quartet by its adaptation to G_{48} required by donor tunneling. The upper $(k=\pm 2)$ state is twofold degenerate and splits into a sextet, because two of the levels remain always twofold degenerate. The allowed transitions and the corresponding nuclear spin statistical weights are shown in Fig. 2. If both β_2 and β_3 differ from zero, it follows that each transition should split into a sextet. What is actually observed in the band at 98.1

cm^{-1} are quartets with an intensity ratio of (approximately) 8:2:4:3. If β_2 is not equal to zero, this result can only be reproduced for a very specific ratio of β_2 and β_3. Without the assumption of such a specific relation, the collapse of sextets into quartets with the observed intensity ratio can only be explained by assuming that β_2 equals zero, both in the ground and the excited state, and that the value of β_3' for the upper state is considerably larger than β_3 for the ground state. From the line spacing of 1.5 MHz of the quartets in the band at 41.1 cm^{-1} one knows already that $\beta_3 = -1.1$ MHz for the ground ($k=0$) state. The observation that the line spacing in the band at 98.1 cm^{-1} is 5 MHz indicates that, indeed, β_3' must be larger than β_3. Quartets with an intensity ratio of 248:54:108:70, which is rather close to the observed ratio, and a line spacing of 5 MHz are obtained with $\beta_3' = -7.5$ MHz. This follows from the transition energies given in the caption of Fig. 2. It also follows that the outermost peaks are actually split by 0.75 MHz, but this splitting is not observable. Furthermore, it is derived from this assignment that the spacing between the central lines of weights 54 and 108 must be larger (by about 1.9 MHz) than the spacings between these lines and the outer lines. Upon careful examination of the quartets in the spectrum of Fig. 2 this is indeed observed. So, we find with reasonable certainty that also for $(D_2O)_3$ the donor tunneling pathway that produces β_2 may be neglected and that a pathway which involves inversion (E^*) and produces the matrix element β_3 is preferred.

IV. CONCLUSION

We have made quantitative calculations on $(H_2O)_3$ and $(D_2O)_3$ with the Hamiltonian derived in paper I for the three-dimensional pseudo-rotation tunneling motion in a rotating trimer. The effects of Coriolis coupling with the overall rotation of the trimer are explicitly taken into account, and the effects of donor tunneling are included through a semi-empirical model. We have also presented new experimental data which show, in particular, that specific levels in the donor tunneling quartets of the band at 87.1 cm^{-1} in $(H_2O)_3$ are further split into doublets, in a manner which occurs normally in a slightly asymmetric rotor with ''axis switching.'' In this case, the doublet splitting occurs only for substates of specific symmetry, however.

Our calculations show, in the first place, that the J-independent terms in the Hamiltonian which contain the operator $\boldsymbol{j}$, the vector sum of the angular momenta associated with the fixed-axis rotations of the monomers, are not negligible. In earlier calculations on pseudo-rotation tunneling[7–9] (without the overall rotation, but with the same *ab initio* potentials) these terms were not included. The main differences between the earlier results and ours are due to a different value of the effective moment of inertia associated with the torsions of the monomers. We have derived an expression for this quantity in paper I; in the earlier calculations it was assumed *ad hoc*.

With the *ab initio* potential of the Van Duijneveldts[14,18] (the DD-potential) we find good agreement with the experimental frequencies for the excitations among the lowest six pseudo-rotation states, with the G_6 labels $k=0,\pm1,\pm2,3$. For the higher excitations the *ab initio* potential of Bürgi *et al.*[15] (the BGLK-potential) yields better results, which is somewhat surprising since this potential gives far too low energies for the lower levels. The lower quality of the DD-potential at higher energies may be caused by its expansion in polynomials; this expansion breaks down for larger values of the torsional angles, and it may already deteriorate for angles which are physically accessible at higher energies.

We can conclude that the results of our quantitative calculations support the qualitative model of paper I. This implies not only that the model gives qualitatively correct energy levels for the lowest six pseudo-rotation states, but also that it yields the correct relative size of the Coriolis coupling matrix elements between these states. All the Coriolis splittings of degenerate levels predicted by the model were actually found and, except in one case, even the relative size of these splittings was given correctly by second order (degenerate) perturbation theory. In that particular case, it was found that the Coriolis splitting of a degenerate state was substantially reduced by (destructive) interference effects between the couplings of its two substates with the higher levels. If we include donor tunneling as well, the resulting splitting patterns for $J>0$ become rather complex, because the (first order) donor tunneling effects have the same order of magnitude as the second order Coriolis shifts.

With the results of these quantitative calculations and the model of paper I, we can interpret all the splittings observed in the high-resolution spectra of $(H_2O)_3$ and $(D_2O)_3$, including their J-dependence. A consistent assignment was given of all the bands measured up to now (except for the band at 82.5 cm^{-1} in $(D_2O)_3$ which was not yet analyzed). The small doublet splittings within the donor tunneling quartets of the band at 87.1 cm^{-1} for $(H_2O)_3$, which are described for the first time in the present paper, are explained. They look like the effect of asymmetry doubling with ''axis switching,'' but occur only for specific symmetries; we find that they are caused by donor tunneling splittings induced through Coriolis mixing.

We find that donor (or bifurcation) tunneling occurs, both in $(H_2O)_3$ and in $(D_2O)_3$, through a pathway that involves inversion, E^*. Another pathway for donor tunneling, which was predicted by *ab initio* calculations[10] to be preferred, is in fact negligible. In a more recent *ab initio* study[24] it was concluded that it is actually very difficult to predict which are the most relevant tunneling pathways by calculations of the potential surface, since the outcome depends sensitively on the level of the calculations. The information that we extract from the spectra, with the help of the group theoretical analysis in paper I and the calculations in the present paper, is unambiguous, however. For $(H_2O)_3$ our conclusion on the preferred donor tunneling pathway is obtained from the observation of ''axis switching'' effects in the band at 87.1 cm^{-1}. For $(D_2O)_3$ it follows, although with somewhat less certainty, from an analysis of the quartet intensity pattern in the band at 98.1 cm^{-1}.

ACKNOWLEDGMENTS

We thank Professor F. B. van Duijneveldt for making available an improved fit of their *ab initio* potential before publication and E. Meijer for communicating his unpublished results. The Nijmegen authors also like to thank Dr. W. L. Meerts for useful discussions. Kun Liu and R. J. Saykally are supported by the Experimental Physical Chemistry Program of the National Science Foundation (Grant No. CHE-9123335).

[1] N. Pugliano and R. J. Saykally, Science **257**, 1937 (1992).
[2] K. Liu, J. G. Loeser, M. J. Elrod, B. C. Host, J. A. Rzepiela, N. Pugliano, and R. J. Saykally, J. Am. Chem. Soc. **116**, 3507 (1994).
[3] K. Liu, M. J. Elrod, J. G. Loeser, J. D. Cruzan, N. Pugliano, M. G. Brown, J. A. Rzepiela, and R. J. Saykally, Faraday Discuss. Chem. Soc. **97**, 35 (1994).
[4] J. D. Cruzan, M. R. Viant, D. D. Lucas, L. B. Braly, and R. J. Saykally (unpublished).
[5] S. Suzuki and G. A. Blake, Chem. Phys. Lett. **229**, 499 (1994).
[6] M. Schütz, T. Bürgi, S. Leutwyler, and H. B. Bürgi, J. Chem. Phys. **99**, 5228 (1993).
[7] W. Klopper and M. Schütz, Chem. Phys. Lett. **237**, 536 (1995).
[8] D. Sabo, Z. Bačić, T. Bürgi, and S. Leutwyler, Chem. Phys. Lett. **244**, 283 (1995).
[9] E. Meijer and F. B. van Duijneveldt (unpublished).
[10] D. J. Wales, J. Am. Chem. Soc. **115**, 11180 (1993).
[11] J. K. Gregory and D. C. Clary, J. Chem. Phys. **102**, 7817 (1995).
[12] J. K. Gregory and D. C. Clary, J. Chem. Phys. **103**, 8924 (1995).
[13] C. Millot and A. J. Stone, Mol. Phys. **77**, 439 (1992).
[14] J. G. C. M. van Duijneveldt-van de Rijdt and F. B. van Duijneveldt, Chem. Phys. Lett. **237**, 560 (1995).
[15] T. Bürgi, S. Graf, S. Leutwyler, and W. Klopper, J. Chem. Phys. **103**, 1077 (1995).
[16] W. Klopper, M. Schütz, H. P. Lüthi, and S. Leutwyler, J. Chem. Phys. **103**, 1085 (1995).
[17] G. Herzberg, *Molecular Spectra and Molecular Structure*, *Vol. II* (Van Nostrand Reinhold, New York, 1945).
[18] J. G. C. M. van Duijneveldt-van de Rijdt and F. B. van Duijneveldt (private communication).
[19] D. T. Colbert and W. H. Miller, J. Chem. Phys. **96**, 1982 (1992).
[20] G. C. Groenenboom and D. T. Colbert, J. Chem. Phys. **99**, 9681 (1993).
[21] G. A. Blake, K. B. Laughlin, R. C. Cohen, K. L. Busarow, D.-H. Gwo, C. A. Schmuttenmaer, D. W. Steyert, and R. J. Saykally, Rev. Sci. Instrum. **62**, 1701 (1991).
[22] K. Liu, R. S. Fellers, M. R. Viant, R. P. McLaughlin, M. G. Brown, and R. J. Saykally, Rev. Sci. Instrum. **67**, 410 (1996).
[23] G. Herzberg, *Molecular Spectra and Molecular Structure*, *Vol. III* (Van Nostrand Reinhold, New York, 1945), p. 268.
[24] T. R. Walsh and D. J. Wales, J. Chem. Soc. Faraday Trans. **92**, 2505 (1996).